

Fig. S1. Krona plots of abundances of microbiome taxonomic units derived from 16S stool sequencing. Graphical overview of relative taxonomic composition of gut microbiomes in the study. Stool samples were collected at baseline (V1), post fasting / one week of DASH (V2) and after three months (V3) intervention and were characterized using 16S sequencing. (A) Fasting + DASH. (B) DASH.

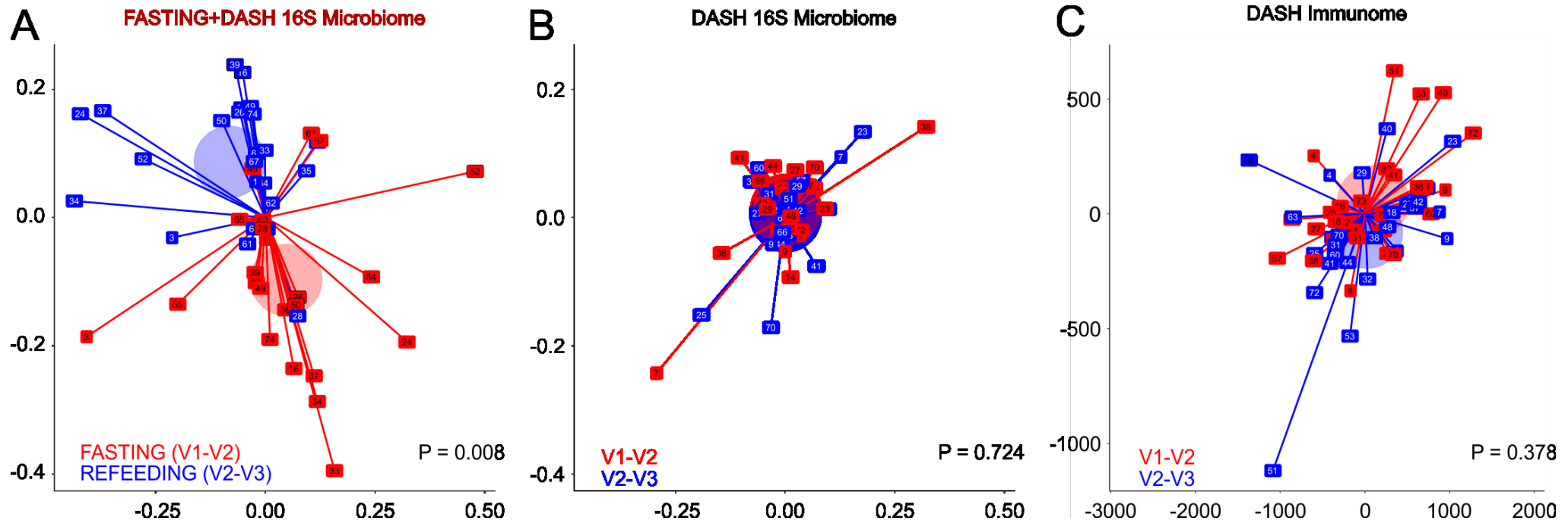


Fig. S2. Changes to the microbiome at the level of 16S OTUs in the FASTING+DASH and DASH groups, and changes to the immunome in the DASH arm. Unconstrained Principal Coordinates graph with first two dimensions shown. Axes show fasting and refeeding deltas in the case of FASTING+DASH (A) and DASH, and V1-V2, V2-V3 deltas in the case of DASH after one-week intervention and three-month. Pseudonym participant ID numbers are shown on the point markers. Transparent circle markers show arithmetic mean position of one week intervention and three-month (A, B). Circles of (D) denote the same like in A and B, but with Euclidean distances.

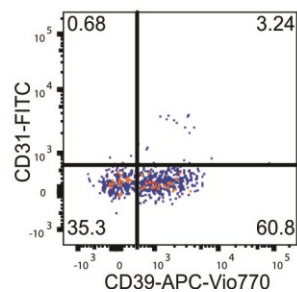
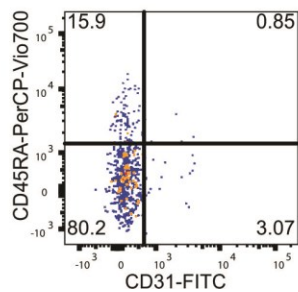
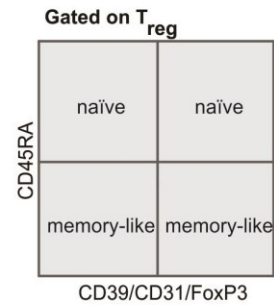
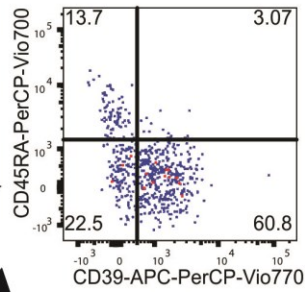
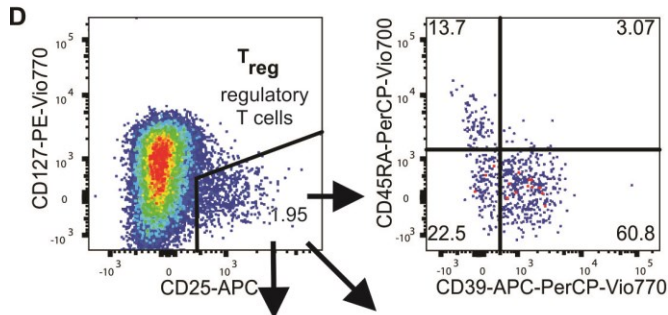
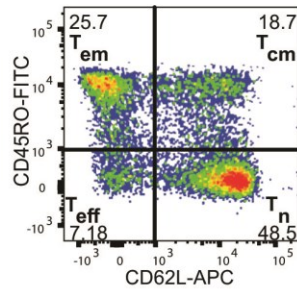
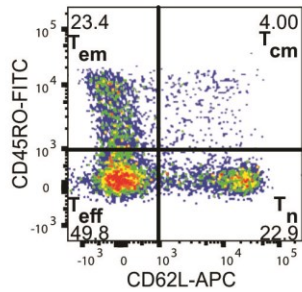
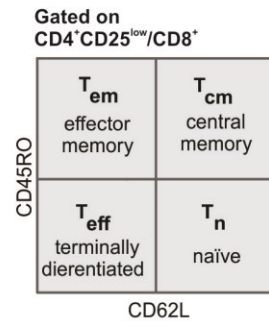
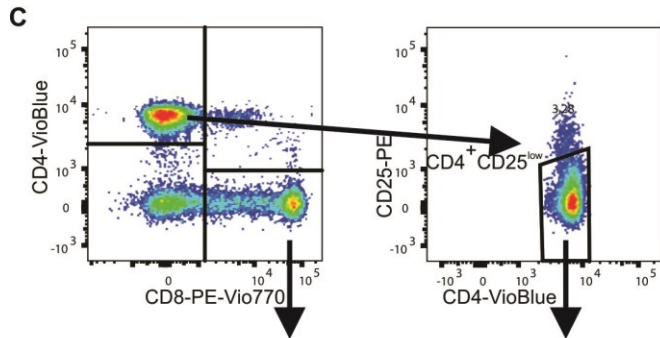
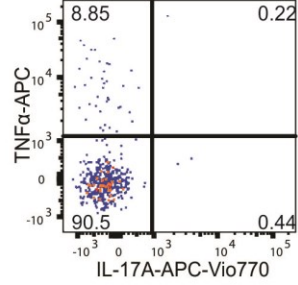
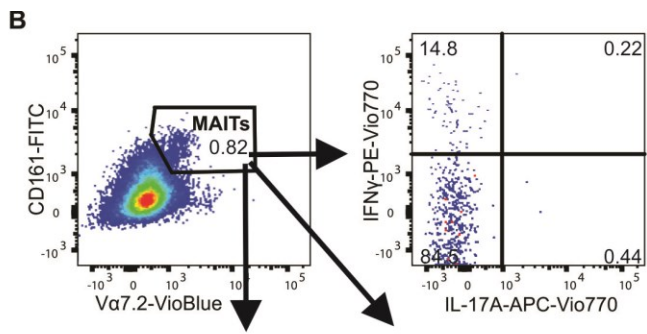
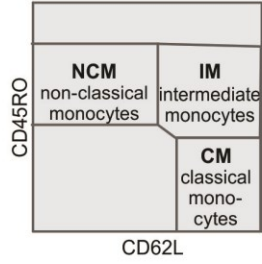
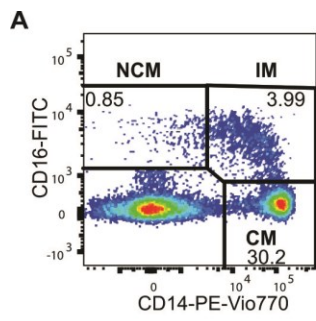
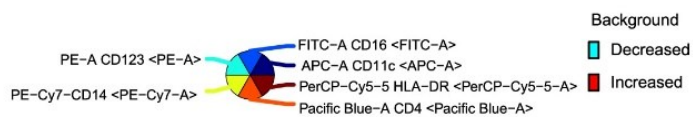
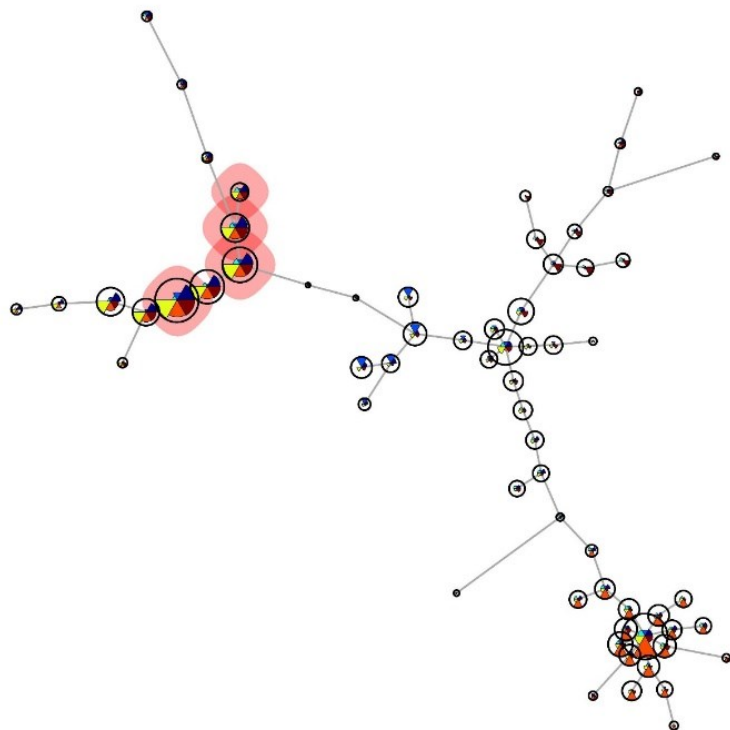
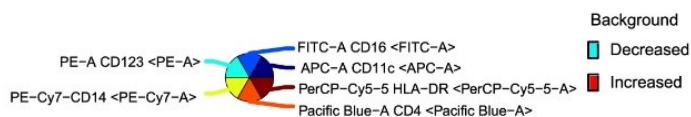
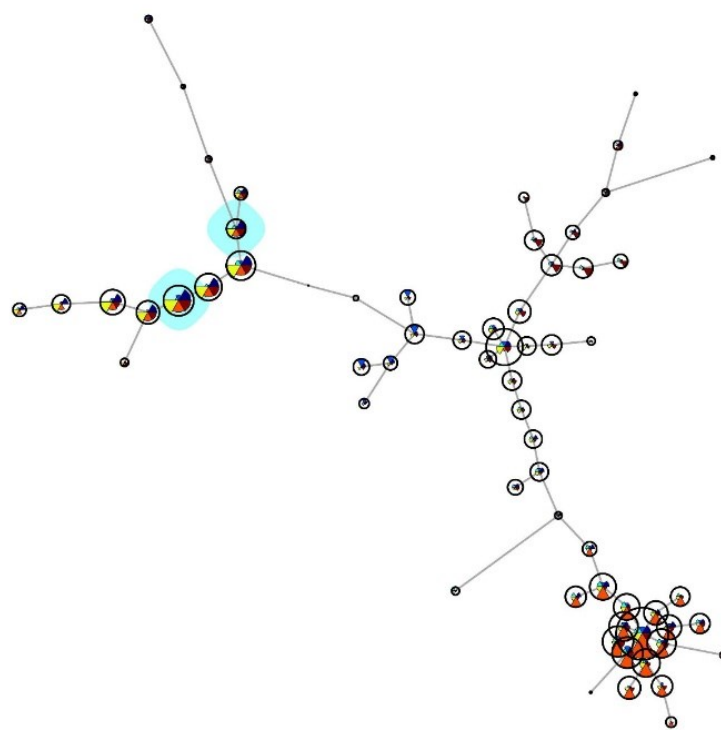


Fig. S3. Gating strategy of monocytes, mucosa-associated invariant T cells, T cell activation and regulatory T cells. Events are shown after gating onto FSC-Area vs. SSC-Area, followed by gating on doublet and dead exclusion. (A) Monocytes were detected from whole peripheral blood mononuclear cell (PBMC) fraction. Monocytes were gated in an HLA-DR⁺ or HLA-DR⁻CD16⁻ subset. Classical, non-classical, and intermediate monocytes were defined as CD14^{high}CD16⁻, CD14^{low}CD16⁺⁺, and CD14⁺CD16⁺, respectively. (B) Mucosa associated invariant T (MAIT) cells were detected in PBMCs depleted of CD4⁺ cells using magnetic microbead sorting. MAITs were defined as CD161⁺TCRV α 7.2⁺CD4-CD3⁺. After restimulation with phorbol 12-myristate 13-acetate (PMA) and ionomycin for 4hrs, MAITs were stained for IL-17A, TNF α , and IFN γ . (C) Plots show cells gated on live events using LIVE/DEAD Fixable Aqua Dead Cell Stain kit, for 405nm. T cell subsets were gated as CD8⁺CD4⁻, CD25⁻CD4⁺CD8⁻, and CD25^{high}CD4⁺CD8⁻. Activation of the T cells was assessed by expression patterns of CD45RO and CD62L. Cells were defined as i) effector memory (Tem): CD45RO⁺CD62L⁻, ii) central memory (Tcm): CD45RO⁺CD62L⁺, iii) naïve (Tn): CD45RO⁻CD62L⁺, iv) terminally differentiated (Teff): CD45RO⁻CD62L⁻, as shown in the sketch to the right. (D) Regulatory T cells (Treg) were defined as CD4⁺CD25^{high}CD127^{low} population in isolated PBMCs. Activation status of the cells was detected by the means of surface markers (CD45RA, CD39, and CD31. Representative plots shown.

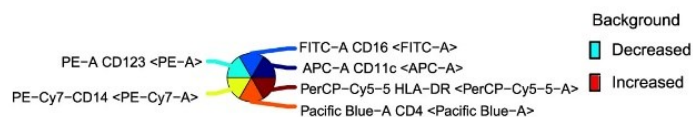
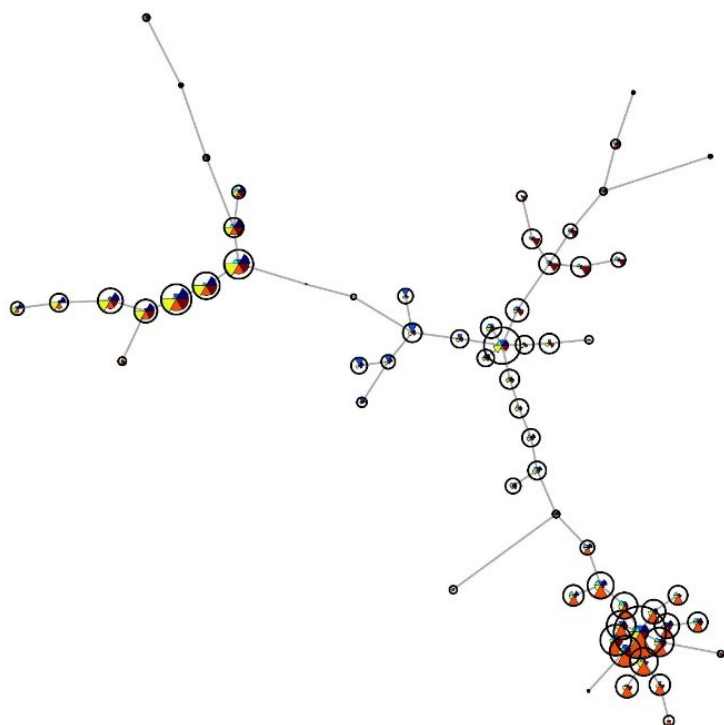
A Baseline (V1) vs. Fasting (V2)



B Fasting (V2) vs. Follow-up (V3)



C Baseline (V1) vs. Follow-up (V3)



D Relative abundance at V1, V2 and V3

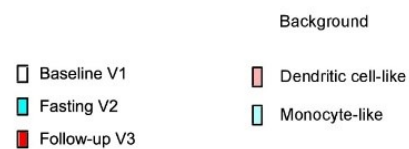
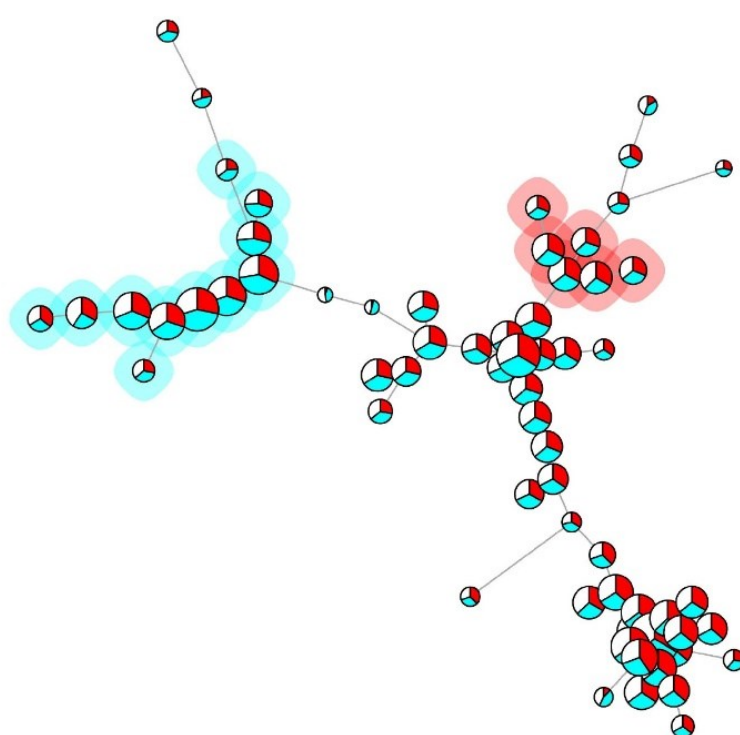


Fig. S4. FlowSOM analysis of monocytes and antigen-presenting cells (APCs) in the fasting arm. Peripheral blood mononuclear cells were labelled with fluorophore conjugated monoclonal antibodies and measured with multicolor flow cytometry. Data was extracted from the viable gate after doublet-exclusion and down sampled to 6000 events. Samples lacking 6000 events from the viable gate were excluded from the analysis. Monocyte like and APC-like nodules were identified and annotated using the CD markers of the respective node. A-C, Increase (red) or decrease (blue) for Fasting effect (A), Refeeding effect (B), and Study effect (C) is shown within the nodes. D, Quantification of the relative changes between all three time points is shown by the pie chart within the nodes. White, blue and red pie slices refer to V1, V2 and V3, respectively. Blue and green background depicts monocytes and antigen-presenting cells, respectively. n = 17 at each time point.

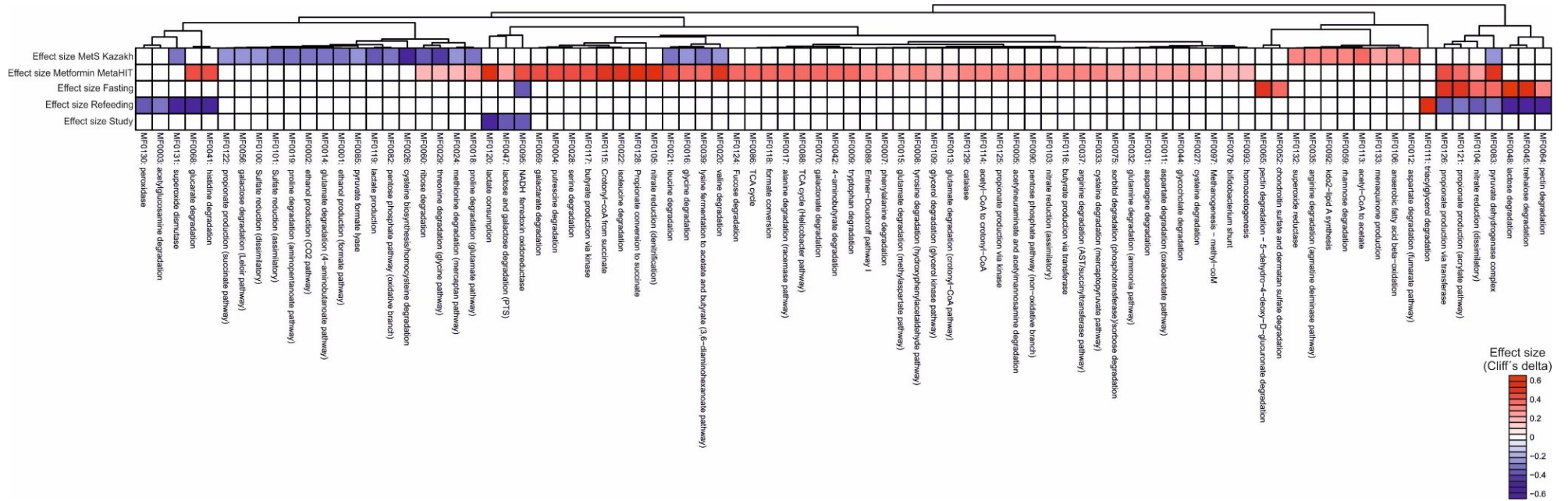


Fig. S5. Microbiome functional potential changes during fasting are similar to those induced by metformin and unlike those characteristic for MetS. Heatmap shows effect sizes (Cliff's delta) of microbiome functional module (GMM) abundance from reanalysis of samples from Forslund et al. (12) and Kushgulova et al. (20), plotted against the original data from our study. Data from Forslund et al. (12) was used to isolate the metformin-associated microbiome functional shifts (using same module definitions as in the present work) for comparison, and Kushgulova et al. (20) data was used to isolate a MetS signal. Fasting, recovery, and overall study effect from our novel data are shown. Blue and red indicate significant (MWU FDR < 0.1 for metformin/MetS status, respectively, post-hoc nested model test for confounder (the other variable) $P < 0.05$) depletion/enrichment in each data set. White indicates non-significant effect or absence of the module in a dataset. Modules significantly different in abundance in the metformin substudy show some overlap with and similar directional changes as in our fasting study, whereas recovery exhibits the opposing pattern. MetS and metformin functional signals are starkly different from one another, however there is little overlap between features altered in MetS and by fasting in our novel data.

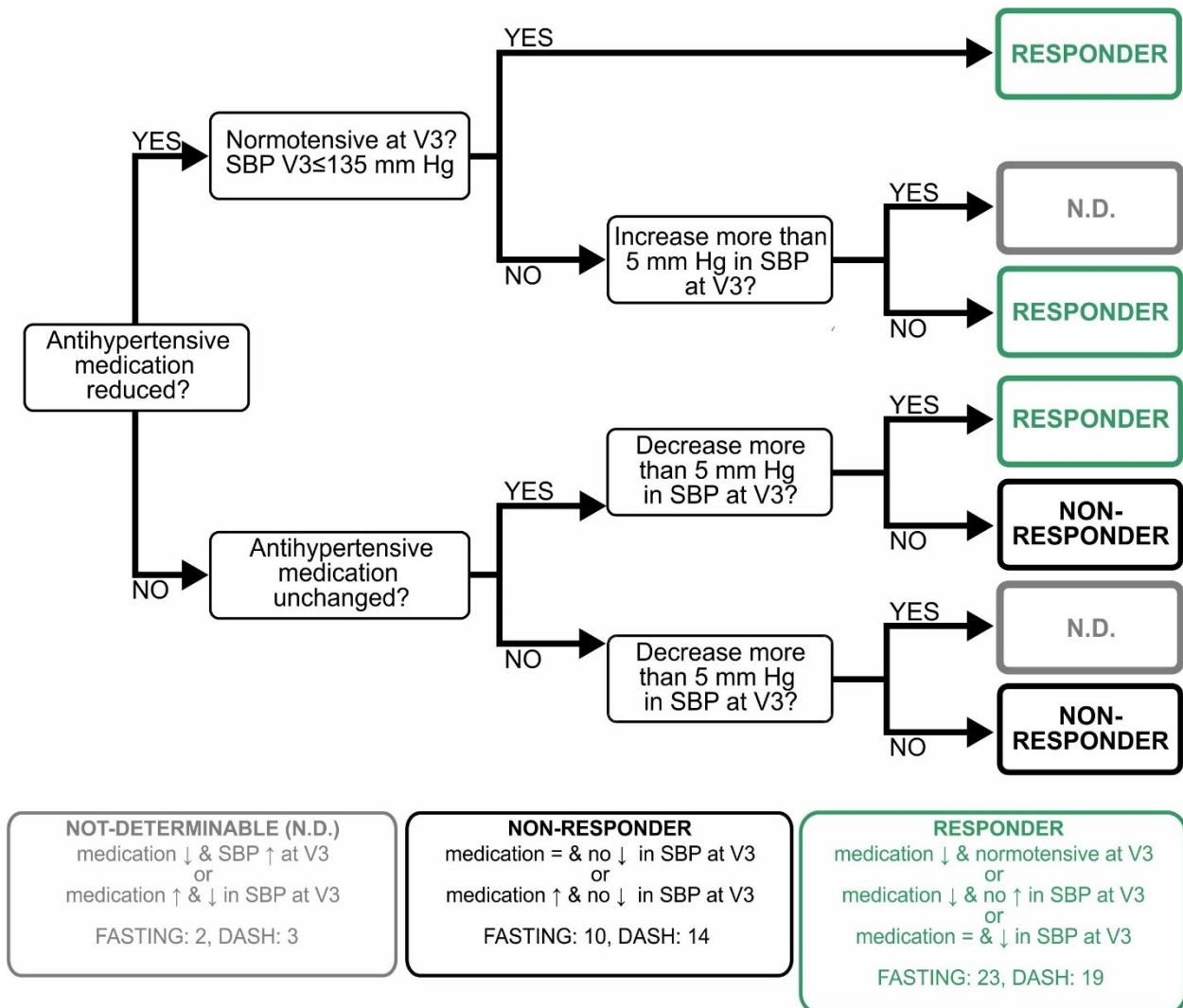


Fig. S6. Decision tree for the determination of blood-pressure responders and non-responders. Individual 24h systolic ambulatory blood pressure (SBP) and individual anti-hypertensive medication at 3 months (V3) was evaluated in relation to baseline (V1) and patients were categorized as responder, non-responder or not determinable. Normotensive SBP was defined as being ≤ 135 mm Hg. Significant change in the SBP was defined as an increase or decrease being ≥ 5 mmHg. Patients were categorized as responders if at V3: i) their anti-hypertensive medication was reduced and SBP was ≤ 135 mm Hg, ii) anti-hypertensive medication was reduced and SBP did not increase significantly, iii) if their anti-hypertensive medication did not change and their SBP significantly decreased (Fasting $n=23$, DASH $n=19$). Patients were categorized as non-responders if at V3: i) their anti-hypertensive medication was not changed and SBP did not decrease significantly, ii) if their anti-hypertensive medication was increased but SBP did not decrease (Fasting $n=10$, DASH $n=14$). Patients were categorized as not-determinable if at V3: i) their anti-hypertensive medication was decreased and SBP significantly increased, ii) their anti-hypertensive medication was increased and SBP significantly decreased (Fasting $n=2$, DASH = 3).

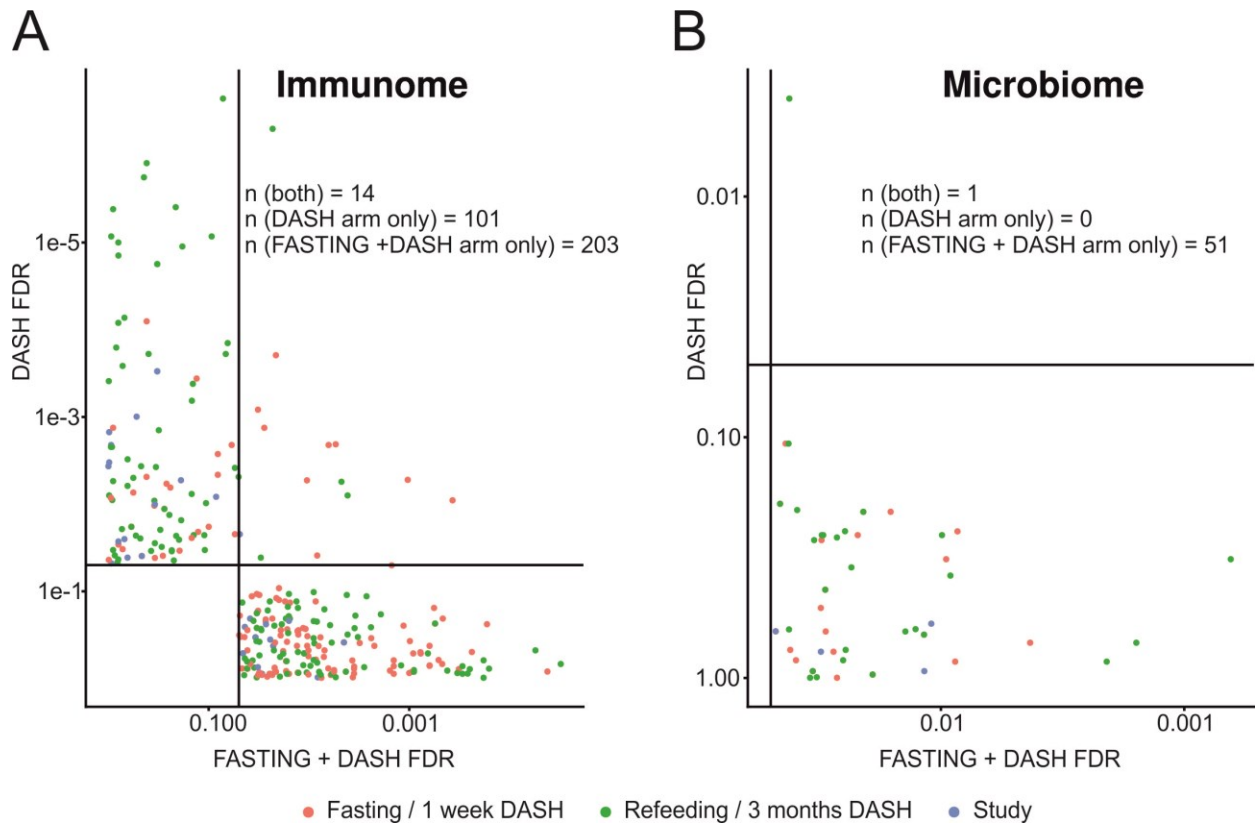


Fig. S7. Fasting and recovery effects are not replicated in an equally powered control cohort, indicating they are intervention-specific. Volcano plots show post-hoc FDR for all features significantly altered in either arm between any two time points in the fasting arm (horizontal axis), compared to the same sample number DASH arm (vertical axis). Point color shows which time point comparison is plotted. Quadrants (formed by the $FDR < 0.05$ thresholds) and summary counts highlight features significantly altered in each dataset for immune cell (A) and microbiome functional or taxonomic (B) features. Only the fasting arm had a significant effect on the microbiome, and while a smaller fraction of immune features are altered in the DASH-only arm, these are largely not significant in the fasting arm.

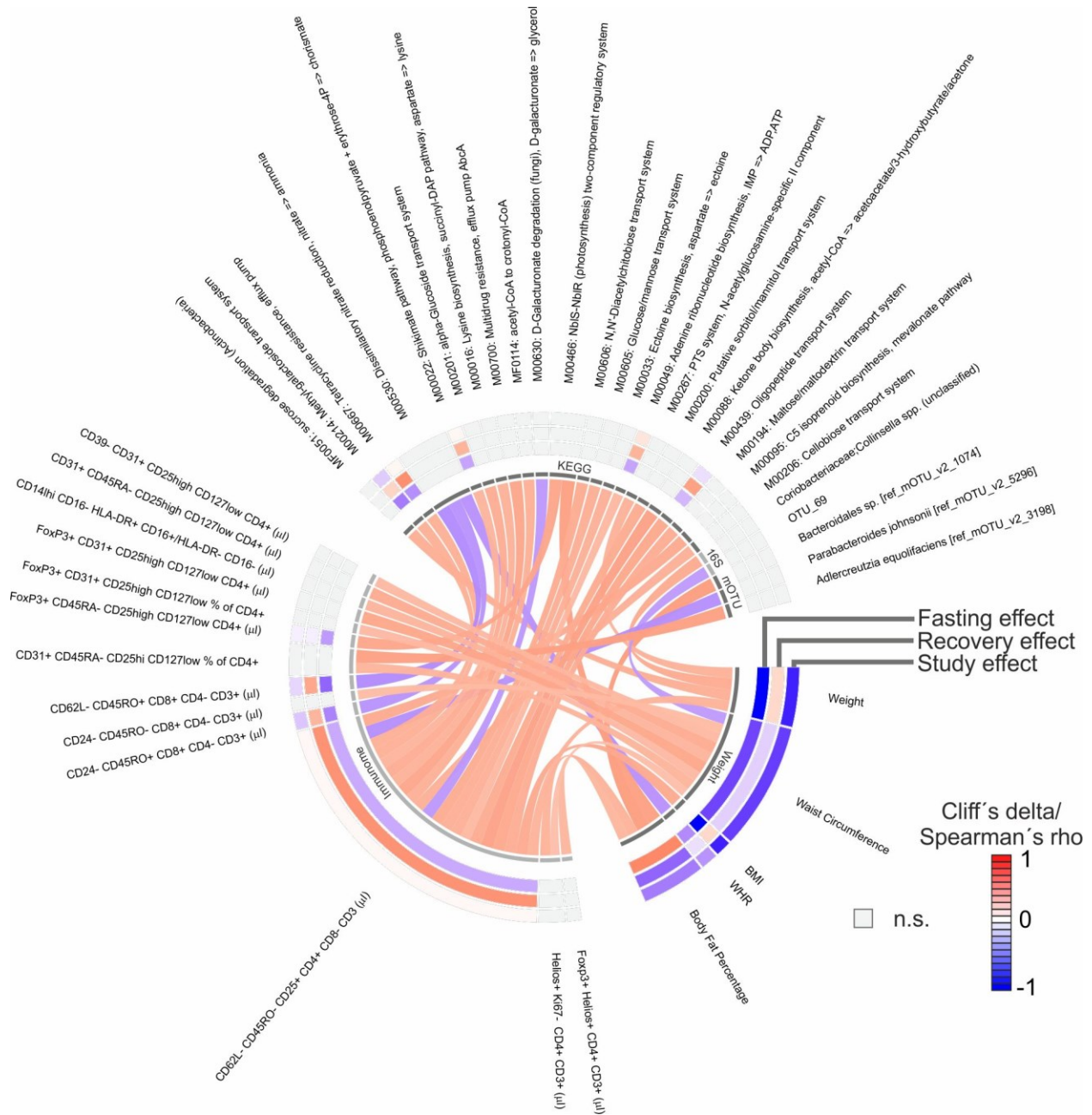
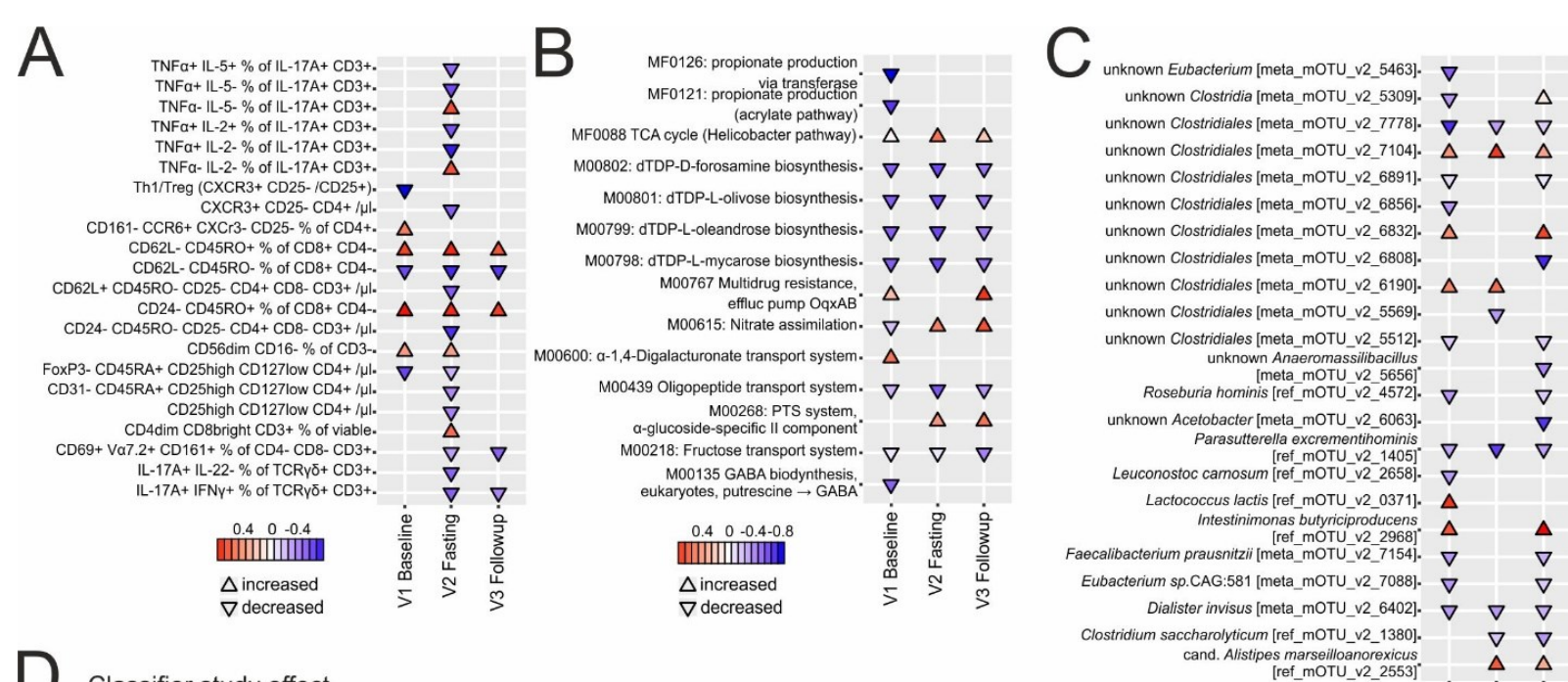


Fig. S8. Association between the immunome, microbiome and body weight-related features. Chord diagram visualizes the interrelation between body weight-related parameters (body weight, waist circumference, BMI, waist-hip ratio (WHR), and body fat percentage), fasting impacted microbiome functional or taxonomic features, and immune cell subsets. Features are shown that form triplets of immune, microbial and phenotype variables where at least two of three correlations are significant (Spearman FDR < 0.05, post-hoc nested model test accounting for same-donor samples < 0.05) in the fasting arm of our cohort, and where in addition one or more feature significantly (drug-adjusted post-hoc FDR < 0.05) are affected by the intervention. Color of the connectors indicates positive or negative correlation (Spearman's rho), color of the cells within the tracks indicates changes upon fasting, refeeding and study effect (Cliff's delta).



D Classifier study effect

Single-subject prediction: 78%

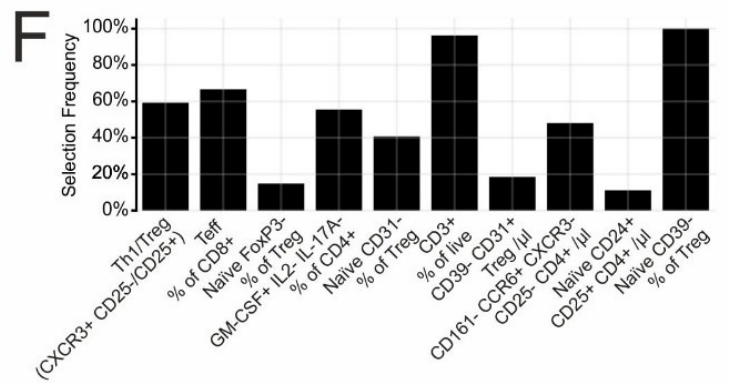
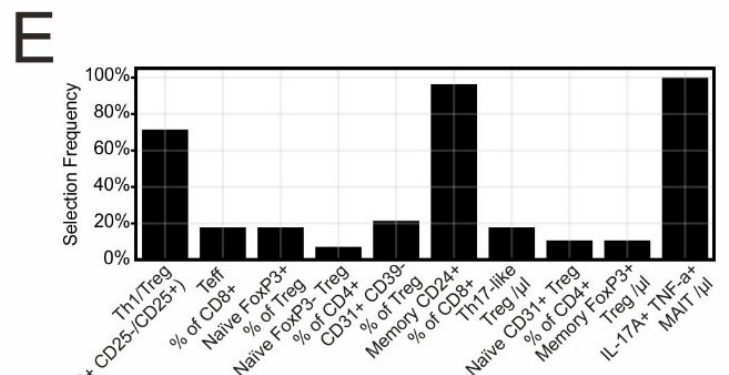
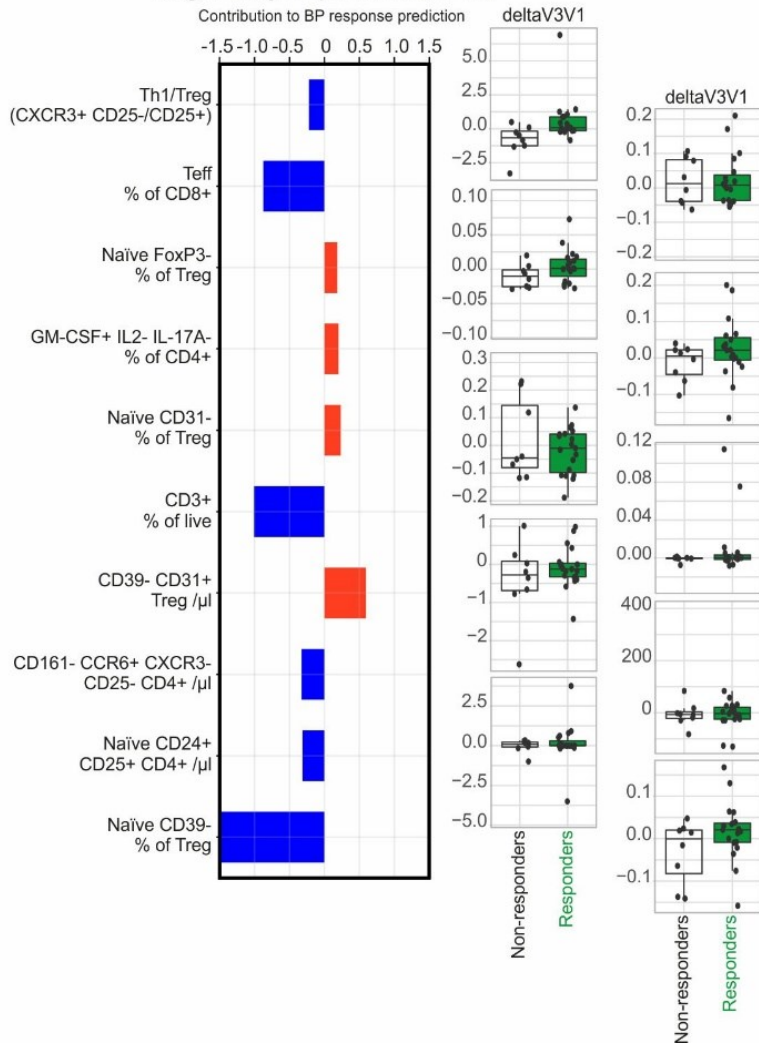


Fig. S9. Long-lasting blood pressure responders and non-responders differ in microbiome and immunome composition. (A-C) Cuneiform plot shows effect sizes (Cliff's delta; hue and marker size shows effect size, marker direction shows sign of effect) of immunome features (A), gut functional profiles using KEGG and GMM (B), and gut taxon abundances assessed using the mOTUv2 framework (C) significantly (posthoc FDR < 0.05) differing between responders and non-responders at the different time points. (D), Prediction model for blood pressure response using the changes of immune features between baseline (V1) and follow-up (V3). Single subject prediction was quantified using a leave-one-out cross-validation approach. Ten immune cell features were used to build up a multivariate logistic-regression algorithm. The bar plots represent the regression in a model with binary output (responder yes=1 vs no=0) for every feature. (E), Selection frequency of the different parameters for the prediction model shown in Fig. 4c over the different classifiers built by using a leave-one-out cross-validation. (F), Selection frequency of the different parameters for the prediction model shown in (D) over the different classifiers built by using a leave-one-out cross-validation. Treg: CD25^{high}CD127^{low}CD4⁺.